# Reduced rich-club connectivity is related to disability in primary progressive MS

Jan-Patrick Stellmann, Sibylle Hodecker, Bastian Cheng, Nadine Wanke, Kim Lea Young, Claus Hilgetag, Christian Gerloff, Christoph Heesen, Götz Thomalla, Susanne Siemonsen

# Reduced rich-club connectivity is related to disability in primary progressive MS

OPEN

Jan-Patrick Stellmann, MD*
Sibylle Hodecker, MD*
Bastian Cheng, MD
Nadine Wanke, MSc
Kim Lea Young, MD
Claus Hilgetag, PhD
Christian Gerloff, MD
Christoph Heesen, MD
Götz Thomalla, MD
Susanne Siemonsen, MD

Correspondence to Dr. Stellmann: j.stellmann@uke.de

## ABSTRACT

**Objective:** To investigate whether the structural connectivity of the brain's rich-club organization is altered in patients with primary progressive MS and whether such changes to this fundamental network feature are associated with disability measures.

**Methods:** We recruited 37 patients with primary progressive MS and 21 healthy controls for an observational cohort study. Structural connectomes were reconstructed based on diffusion-weighted imaging data using probabilistic tractography and analyzed with graph theory.

**Results:** We observed the same topological organization of brain networks in patients and controls. Consistent with the originally defined rich-club regions, we identified superior frontal, precuneus, superior parietal, and insular cortex in both hemispheres as rich-club nodes. Connectivity within the rich club was significantly reduced in patients with MS ($p = 0.039$). The extent of reduced rich-club connectivity correlated with clinical measurements of mobility (Kendall rank correlation coefficient $\tau = -0.20$, $p = 0.047$), hand function ($\tau = -0.26$, $p = 0.014$), and information processing speed ($\tau = -0.20$, $p = 0.049$).

**Conclusions:** In patients with primary progressive MS, the fundamental organization of the structural connectome in rich-club and peripheral nodes was preserved and did not differ from healthy controls. The proportion of rich-club connections was altered and correlated with disability measures. Thus, the rich-club organization of the brain may be a promising network phenotype for understanding the patterns and mechanisms of neurodegeneration in MS. *Neurol Neuroimmunol Neuroinflamm* 2017;4:e375; doi: 10.1212/NXI.0000000000000375

## GLOSSARY

**APL** = average shortest path length; **EDSS** = Expanded Disability Status Scale; **FDR** = false discovery rate; **FSL** = functional imaging software library; **HC** = healthy control; **MANCOVA** = multivariate analysis of covariance; **MSFC** = multiple sclerosis functional composite; **NHPT** = Nine-Hole Peg Test; **PPMS** = primary progressive MS; **RRMS** = relapsing-remitting MS; **SDMT** = Symbol Digit Modalities Test; **SWI** = small-world index; **T25FW** = timed 25-foot walk.

MS is the most common autoimmune disease of the CNS, and persistent inflammation as well as chronic progressive neurodegeneration in the brain and spinal cord leads to accumulation of disability.[1,2] MRI is currently the best available surrogate marker of MS pathology.[3] MRI also permits the use of probabilistic tractography, which allows investigating the integrity of structural connections in the brain.

The human brain can be considered as a network and the network's topology can be studied by graph theory. The network perspective may offer new insights into disease-specific processes such as neurodegeneration and has been applied to several neuropsychiatric diseases.[4,5] Recent studies recognized an essential topological feature of the human connectome. The brain network is organized into a so-called rich-club and peripheral nodes.[6,7] The rich-club brain regions are more densely interconnected than expected by chance and form a prominent subnetwork of the

Supplemental data at Neurology.org/nn

*These authors contributed equally to this work.

From the Institut für Neuroimmunologie und Multiple Sklerose (INIMS) (J.-P.S., S.H., N.W., K.L.Y., C.G., C. Heesen, S.S.), Klinik und Poliklinik für Neurologie (J.-P.S., S.H., B.C., N.W., K.L.Y., C. Heesen, G.T.), Institute of Computational Neuroscience (C. Hilgetag), and Department of Diagnostic and Interventional Neuroradiology (S.S.), University Medical Center Hamburg-Eppendorf, Germany.

Funding information and disclosures are provided at the end of the article. Go to Neurology.org/nn for full disclosure forms. The Article Processing Charge was funded by the authors.



  

brain. They are considered to have a guiding function controlling integration and information flow in the brain network. The rich-club architecture assures a highly efficient structural and functional network organization,[8] but might be vulnerable in brain diseases. Altered rich-club connectivity has been observed in schizophrenia,[9] migraine,[10] or dementia.[11]

MS can also be considered as a network disorder leading to focal and global impairment of the brain network.[5,12–16] However, the rich-club organization in patients with MS has not been analyzed. We aimed to analyze the network topology of structural connectomes of patients with a predominantly neurodegenerative disease course. Primary progressive MS (PPMS) shows less and more diffuse inflammatory disease activity than relapsing-remitting MS (RRMS), and clinical assessment in most cases is not blurred by superimposed relapses. Therefore, PPMS might be taken as a candidate model for investigating long-term changes of brain network architecture in MS. We hypothesized that the connectome architecture of patients with PPMS differs from that of healthy controls (HCs), in particular with respect to the rich-club organization, and that these changes might be associated with disability measures.

## METHODS

**Patients and controls.** Patients were eligible for this observational cohort study if they were diagnosed with PPMS according to the McDonald criteria 2010[17] and had an Expanded Disability Status Scale (EDSS) score of ≤7.0. Patients (n = 37) obtained structural MRI and completed a modified multiple sclerosis functional composite (MSFC) test battery,[18] including the timed 25-foot walk (T25FW, short distance walking speed), the Nine-Hole Peg Test (NHPT, dominant and nondominant fine motor hand function), and the Symbol Digit Modalities Test (SDMT, information processing), which is considered as a simple-to-administer, less stressful, and valid substitute for the MSFC standard Paced Auditory Serial Addition Test.[19] We recruited 21 HCs matched by age and sex and applied the same MRI protocol.

**Standard protocol approvals, registrations, and patient consents.** Participants were recruited at our MS day hospital (2012–2016), provided written informed consent, and the Institutional Review Board (ethics committee of the Hamburg Chamber of physicians, PV3961/PV4405) approved the study.

**Image processing and reconstruction of brain networks.** Briefly, the MRI protocol included a T1-weighted sequence (0.9 × 0.9 × 0.9 mm), a T2 sequence (0.5 × 0.5 × 3.0 mm), and diffusion tensor imaging (single-shell, 20 directions with noncollinear diffusion gradients [b = 1,000 s/mm$^2$] and 1 nondiffusion-weighted b0 image, 1.9 × 1.9 × 2.0 mm). Images were processed with the functional imaging software library (FSL) and FreeSurfer software.[20] For each participant, the gray matter was parcellated into 34 cortical regions per hemisphere and 8 subcortical regions based on the Destrieux atlas. Subcortical white matter regions corresponding to the 34 cortical regions were used for FSL probabilistic tracking with crossing fibers (probtrackx). Based on the number of streamlines reaching from one FreeSurfer region to another, 2 different kinds of networks were defined. First, we used the average number of streamlines (forward/backward) between every 2 regions as edge weight to construct weighted networks $G^{raw}$. Second, binary networks (0 = unconnected and 1 = connected) were constructed ($G^{bin}$) based on $G^{raw}$, by discarding connections with a number of streamlines below a given threshold (e.g., 80% of maximum connection strength). This procedure meets the standard to avoid totally connected networks and reduces the number of edges to the most prominent and strongest connections. However, there is no consensus, how to define this threshold.[5,21] We investigated the small-world index (SWI) of individual $G^{bin}$ at thresholds from 2.5% to 97.5% in steps of 2.5% to determine a suitable common cutoff for all participants. The best threshold was defined as the highest cutoff with a median SWI above 1 (indicating small-world features) but low variance of the SWI (no major bias of this fundamental network feature). For a detailed description, see supplemental material at Neurology.org/nn.

**Graph metrics.** Global parameters included strength ($G^{raw}$), average shortest path length (APL, $G^{bin}$), global efficiency ($G^{bin}$), clustering coefficient ($G^{bin}$) and weighted clustering coefficient ($G^{raw}$), and arithmetic mean method. In addition, we computed the node-specific degree ($G^{bin}$), betweenness centrality ($G^{bin}$), and strength ($G^{raw}$).

**Rich club.** Rich-club nodes are more densely interconnected than expected by chance (compared with random networks). Thus, the rich club of a given network can be defined by top-ranking nodes based on degree or strength. Eight cortical regions have been identified as rich-club hubs in healthy individuals, which we used as an a priori–defined rich club: superior frontal, precuneus, superior parietal, and insular cortex in both hemispheres.[6] First, we were interested if node-specific measures identify the predefined rich-club nodes in terms of high strength, degree, and betweenness in patients and controls. We then implemented a formal test of the rich-club organization[22] and investigated whether alternative rich-club definitions (accounting, e.g., for individual variability) might perform better than the original definition (see supplemental material). We computed the connectivity within the rich-club, between rich-club and peripheral nodes (so-called feeder connections), and between peripheral nodes. In addition to the absolute values, rich club, feeder, and peripheral connectivity were each divided by the total connectivity of the individual network. The latter approach was chosen to account for the presumed generalized loss of connectivity in patients with PPMS. The measures were then compared by their ability to distinguish between patients with PPMS and HCs, and their association with clinical outcomes and global MRI volumes.

**Statistics.** We performed descriptive statistics according to the nature of the data as mean with SD or as frequencies and/or percentages. Differences between patients and controls were assessed by the Student $t$ test for continuous data and the $\chi^2$ test for categorical data. The distribution of connectivity on rich club, feeder, and peripheral connections was compared by multivariate analysis of covariance (MANCOVA adjusting for age, sex, T2 lesion volume, and total connectivity). To depict the direction of changes, relative connectivity in the different compartments was further analyzed by $t$ tests. To

**Table 1** Descriptive statistics

| | PPMS (n = 39) | HCs (n = 21) | p Value |
|---|---|---|---|
| Female/male, n | 9/28 | 9/12 | 0.242 |
| Age, y | 52.2 (7.9) | 50.4 (6.9) | 0.373 |
| Disease duration, y | 7.6 (5.3) | | |
| Brain volume, $mm^3$ | 1,463,659 (58,775) | 1,511,942 (53,783) | 0.003 |
| White matter volume, $mm^3$ | 764,112 (34,912) | 773,561 (34,912) | 0.310 |
| Gray matter volume, $mm^3$ | 699,547 (38,083) | 738,380 (35,898) | <0.001[a] |
| T1 lesion volume, $mm^3$ | 4,812 (6,376) | | |
| T2 lesion volume, $mm^3$ | 6,406 (7,612) | | |
| EDSS | 3.5 (1.5–7) | | |
| SDMT | −0.7 (1.1) | | |
| T25FW, s | 6.4 (3.4) | | |

Abbreviations: PPMS = primary progressive MS; HC = healthy control (disease duration since first symptoms, tissue and lesion volumes normalized based on SIENAX results); EDSS = Expanded Disability Status Scale; SDMT = Symbol Digit Modalities Test (SDs compared with age, sex, and education-matched normalized data); T25FW = timed 25-foot walk (mean from 2 trials).
Data presented as mean (SD) or median (range). Except from sex ($\chi^2$ test), group differences were compared with the Student *t* test.

account for nonnormal distribution of data, the association between variables was investigated nonparametrically by computing 1-sided Kendall correlation coefficient τ. Post hoc, we compared the predictive value of rich-club connectivity for clinical outcomes with multivariate linear regression. We used analysis of variance to compare unadjusted models with models adjusted for brain volume and T2 lesion volume. *p* Values below 0.05 were considered statistically significant. False discovery rate (FDR) was used to correct for multiple testing. All analyses were performed with Statistics in R 3.2.3, including the igraph and tnet packages.[23,24]

## RESULTS

**Cohort and threshold selection.** Table 1 summarizes descriptive statistics. The mean age of patients with PPMS was 52.2 years and did not differ from HCs (50.4, $p = 0.282$). Disease duration since first symptoms was 7.7 years, and a median EDSS of 3.5 (range 1.5–7) indicated a moderate disability. Brain volume was lower in patients ($p = 0.003$).

Stepwise thresholding of $G^{raw}$ networks increased the SWI of networks only if higher cutoffs were applied (figure e-1). Only with a threshold above 95%, the median SWI was above borderline values. However, we observed in cutoffs above 82.5%, an increase of the variability and several outliers in patients and controls. We interpreted this finding as artificial noise in the data and, therefore, decided to construct $G^{bin}$ based on the highest threshold with acceptable variability, which was 82.5%.

**Global graph metrics.** Global network metrics are presented in table 2. There was no difference between patients with PPMS and controls in terms of total connectivity ($p = 0.340$) or any other graph metric. The association between global graph metrics, MRI volumes, and clinical data is summarized in table 3. Although age, T1, and T2 lesion volumes did not correlate with graph metrics, strength decreased with longer disease duration ($\tau = -0.30$, $p = 0.005$), whereas APL increased ($\tau = 0.23$, $p = 0.027$) with longer disease duration. APL correlated inversely with white matter volume ($\tau = -0.21$, $p = 0.032$) and global efficiency decreased accordingly ($\tau = 0.23$, $p = 0.025$). Walking speed (T25FW) was associated with strength ($\tau = -0.28$, $p = 0.009$) and APL ($r = 0.28$, $p = 0.011$). The association between strength and disease duration, respectively, T25FW, and the correlation between APL and T25FW remained after FDR correction.

**Rich club.** A priori–defined rich-club nodes showed the highest betweenness of all nodes (figure 1), which indicates that their role as an important junction within the networks was preserved. These nodes also ranked within the top 9 nodes based on strength and

**Table 2** Graph metrics: patients and controls

| | PPMS (n = 39) | | HCs (n = 21) | | PPMS vs HCs | |
|---|---|---|---|---|---|---|
| | $G^{raw}$ | $G^{bin}$ | $G^{raw}$ | $G^{bin}$ | $G^{raw}$ | $G^{bin}$ |
| Graph strength | 2,625,250,401 (506,437,884) | 2,463,142,190 (499,636,345) | 2,660,851,915 (383,876,086) | 2,494,621,338 (378,863,703) | 0.764 | 0.788 |
| Average shortest path length | 1.03 (0.02) | 2.17 (0.1) | 1.03 (0.02) | 2.16 (0.07) | 0.876 | 0.438 |
| Global efficiency | 2.23 (0.02) | 1.1 (0.07) | 2.23 (0.02) | 1.12 (0.07) | 0.876 | 0.130 |
| Clustering coefficient | 0.97 (0.01) | 0.51 (0.02) | 0.97 (0.01) | 0.51 (0.01) | 0.826 | 0.058 |
| Clustering coefficient weighted | 0.99 (0.01) | 0.61 (0.02) | 0.99 (0) | 0.60 (0.02) | 0.838 | 0.051 |
| Small-world index | 2.12 (0.03) | 2.04 (0.14) | 2.12 (0.03) | 2.00 (0.09) | 0.800 | 0.210 |

Abbreviations: $G^{bin}$ = binary networks; $G^{raw}$ = weighted networks; HC = healthy control; PPMS = primary progressive MS.
Data presented as mean (SD). Comparison of cohorts by the Student *t* test.

**Table 3** Association of global graph metrics, MRI volumes, and clinical data in PPMS

| | Strength | Average shortest path length | Efficiency | Clustering | Weighted clustering |
|---|---|---|---|---|---|
| **Age** | −0.13 (0.140) | 0.01 (0.484) | −0.08 (0.261) | 0.03 (0.602) | −0.03 (0.408) |
| **Disease duration since diagnosis** | −0.30 (0.005)[a,b] | 0.23 (0.027)[a] | −0.17 (0.077) | −0.12 (0.158) | −0.11 (0.178) |
| **Brain volume** | 0.06 (0.297) | −0.14 (0.118) | 0.08 (0.254) | −0.12 (0.860) | −0.12 (0.848) |
| **White matter volume** | 0.15 (0.098) | −0.21 (0.032)[a] | 0.23 (0.025)[a] | −0.1 (0.815) | −0.11 (0.829) |
| **Gray matter volume** | 0.01 (0.495) | −0.05 (0.344) | −0.05 (0.666) | −0.11 (0.835) | −0.12 (0.860) |
| **T1 hypointense lesion volume** | 0.02 (0.567) | 0.14 (0.123) | −0.06 (0.297) | 0.13 (0.877) | 0.18 (0.943) |
| **T2 hyperintense lesion volume** | −0.05 (0.344) | 0.19 (0.051) | −0.08 (0.262) | 0.02 (0.567) | 0.05 (0.666) |
| **EDSS** | −0.05 (0.349) | 0.09 (0.231) | −0.04 (0.359) | 0.08 (0.744) | 0.06 (0.680) |
| **T25FW** | −0.28 (0.009)[a,b] | 0.28 (0.011)[a,b] | −0.13 (0.146) | −0.01 (0.482) | −0.13 (0.140) |
| **SDMT** | −0.08 (0.738) | −0.16 (0.088) | −0.04 (0.635) | −0.15 (0.884) | −0.15 (0.889) |
| **NHPT dominant hand** | 0.03 (0.593) | 0.13 (0.136) | −0.09 (0.216) | 0.04 (0.633) | 0.08 (0.743) |
| **NHPT nondominant hand** | 0.19 (0.948) | 0.02 (0.43) | 0.14 (0.887) | 0.19 (0.945) | 0.26 (0.987) |

Abbreviations: EDSS = Expanded Disability Status Scale; NHPT = Nine-Hole Peg Test; PPMS = primary progressive MS; SDMT = Symbol Digit Modalities Test; T25FW = timed 25-foot walk.
Associations measured with Kendall $\tau$, $p$ values in brackets.
[a] $p$ Values below 0.05.
[b] False discovery rate–corrected $p$ values below 0.05.

degree (figures e-2 and e-3). Overall, the large-scale organization of the connectomes did not differ between patients with PPMS and HCs. The order of nodes was highly correlated between patients and controls, based on strength ($r = 0.99$, $p = 0.001$), degree ($r = 0.99$, $p < 0.001$), and betweenness ($r = 0.92$, $p < 0.001$). Formal testing confirmed the rich-club organization in average connectomes of patients and controls (figure e-4).

For the a priori–defined rich club, absolute connectivity strength was lower in patients with PPMS than that in controls ($p = 0.038$, FDR-corrected $p = 0.114$). The absolute strength of feeder and peripheral connectivity did not differ ($p = 0.317$ and $p = 0.474$, FDR-corrected both $p = 0.474$). Corrected for total connectivity, T2 lesion volume, age, and sex, we observed an altered distribution of connectivity between rich club, feeder, and periphery in patients with PPMS (MANCOVA $p = 0.011$): pairwise T tests revealed that the percentage of connections within the rich-club, that is, the relative rich-club connectivity, was reduced in patients ($p = 0.013$, FDR-corrected $p = 0.039$), whereas peripheral connectivity was relatively increased in patients than that in controls ($p = 0.040$, FDR-corrected $p = 0.060$, figure 2, A–C).

Absolute rich-club connectivity as well as proportional distribution of connections between the rich club and periphery was not associated with sex, age, disease duration, or T1 lesion volume. By contrast, relatively lower rich-club connectivity and higher peripheral connectivity were associated with increasing T2 lesion load ($\tau = -0.21$, $p = 0.034$) and lower gray matter volumes ($\tau = 0.21$, $p = 0.037$). Relatively lower rich-club connectivity was associated with NHPT (nondominant: $\tau = -0.26$, $p = 0.014$) and T25FW ($\tau = -0.20$, $p = 0.047$). An increased relative peripheral connectivity was instead linked to lower cognitive performance on the SDMT ($\tau = -0.20$, $p = 0.049$). FDR-corrected $p$ values remained significant for NHPT and relative rich-club connectivity. Post hoc, an adjustment for brain volume and T2 lesions did not improve the predictive value of rich-club connectivity for T25FW performance ($p = 0.283$). Concerning NHPT and SDMT, the adjustment for brain volume and T2 lesions performed better than the simple models (both $p < 0.001$). Alternative rich-club definitions did not show a better ability to discriminate between patients with PPMS and HCs, nor were they more closely associated with disability (table e-1).

**DISCUSSION** The rich-club organization of the human connectome has been identified as a fundamental feature of brain networks.[6] Here, we investigated for the first time how the rich-club organization of the human structural connectome is affected in patients with PPMS. Generally, we observed a preserved rich-club organization in patients with PPMS. However, compared with HCs, the connectivity within the rich club was reduced. In addition, lower rich-club connectivity was associated with higher disability.

**Figure 1** **Node-specific graph metrics: Betweenness**

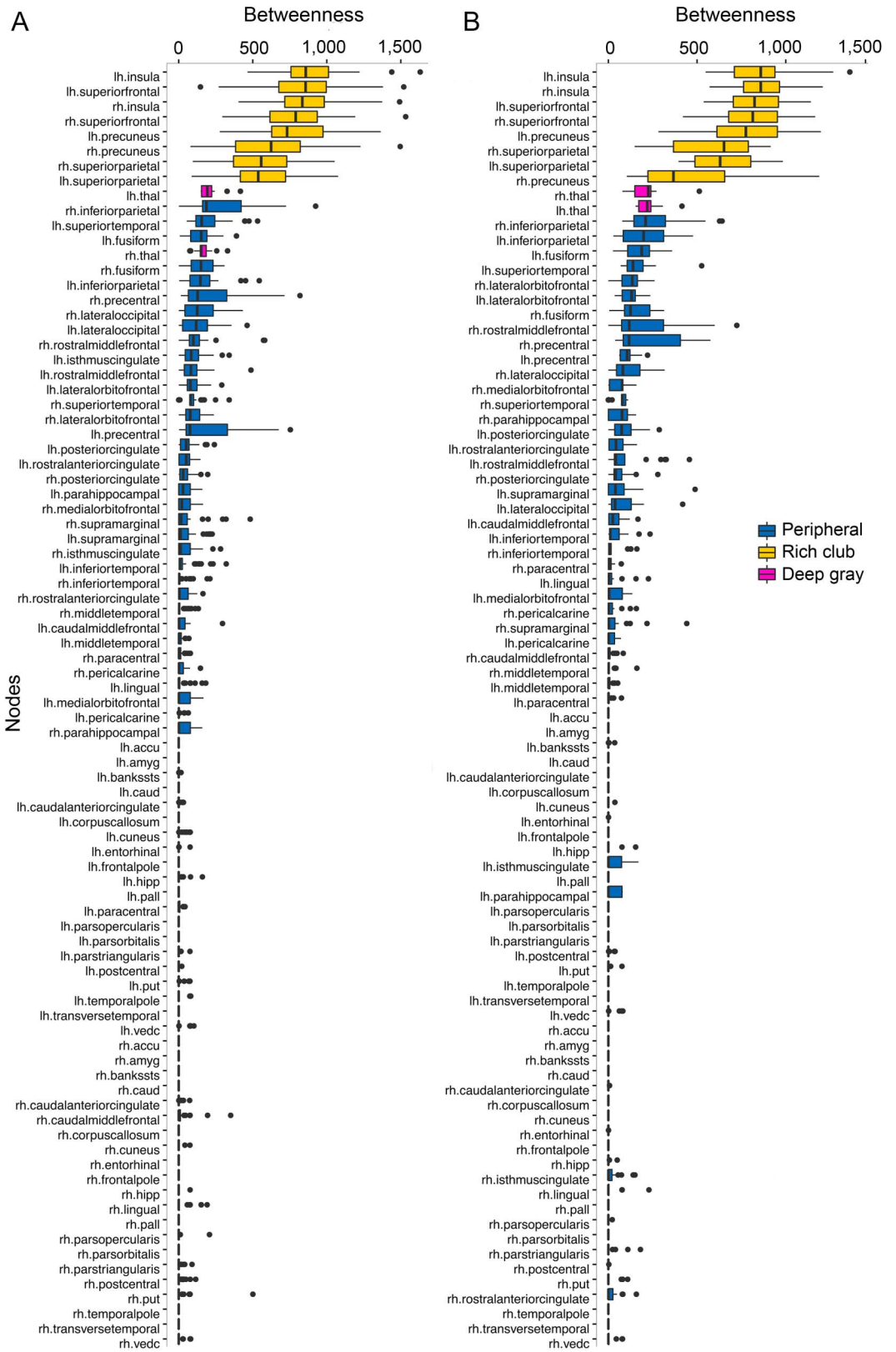


Boxplots ordered by median values of nodes of $G^{bin}$. (A) Healthy controls and (B) primary progressive MS.

Based on the weighted rich-club effect, we confirmed the rich-club organization in controls and patients. The nodes forming the rich club in controls did not differ from those in moderately disabled patients with PPMS. Although the global connectivity was lower in patients, the fundamental organizational

**Figure 2** **Rich-club connectivity**

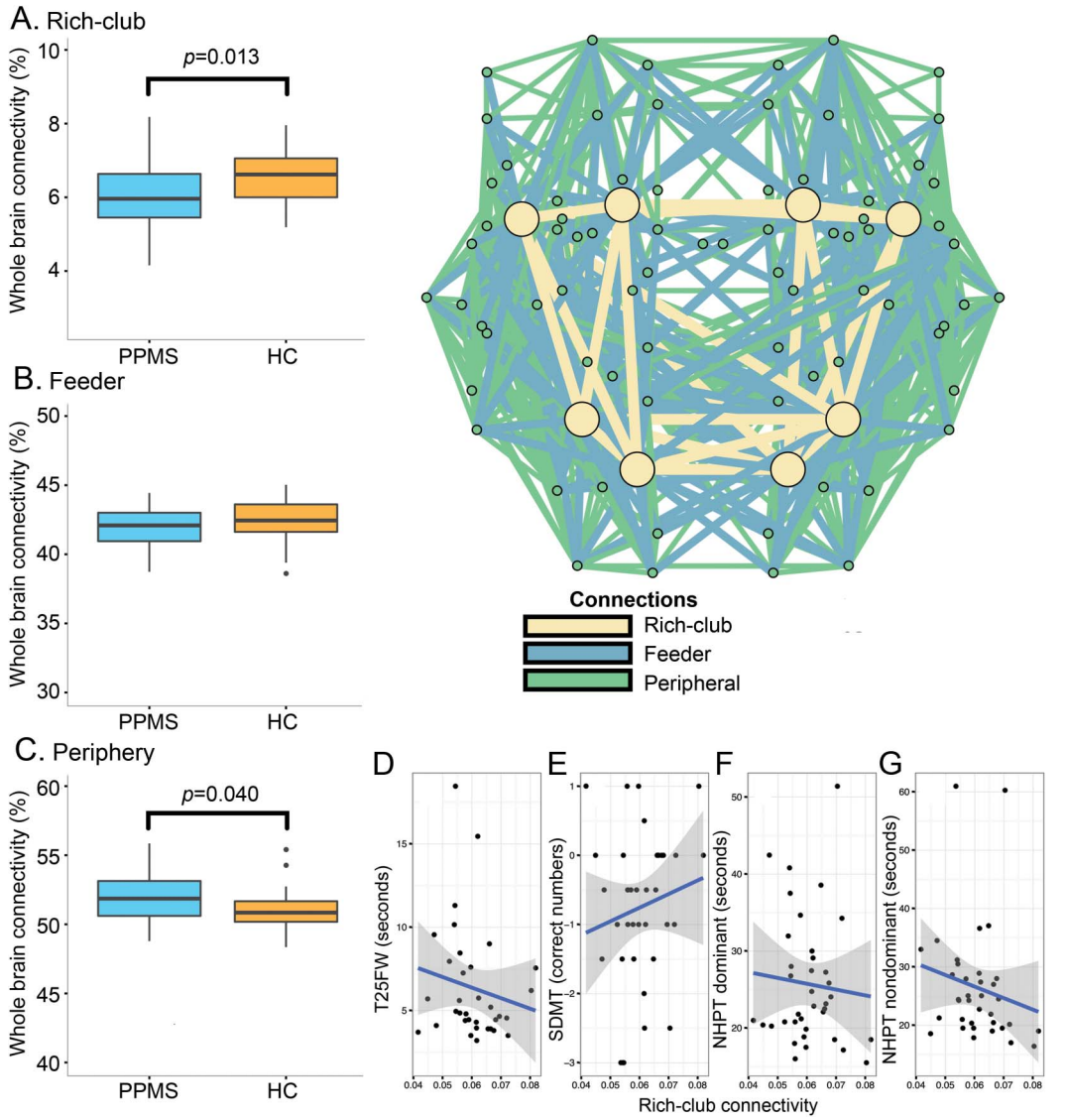


Schematic representation of the rich-club organization in average primary progressive MS (PPMS) connectomes (top right). Boxplots show differences between PPMS (blue) and healthy controls (HCs) (orange) in relative connectivity within the rich club (A), for feeders (B), and within the periphery (C). Dotplots show association between relative rich-club connectivity and (D) T25FW = timed 25-foot walk, (E) SDMT = Symbol Digit Modalities Test, (F) NHPT = Nine-Hole Peg Test dominant hand, and (G) NHPT nondominant hand. Lines and colored areas represent regression estimates and their confident intervals. For details, see Methods and Results sections.

principles did not seem to be affected. Superior frontal, precuneus, superior parietal, and insular cortex in both hemispheres formed the rich club in patients and controls in line with the originally defined rich-club nodes.[6] The dominance of these nodes was consistent across different nodal graph metrics.

The absolute number of rich-club connections was lower in patients than that in controls, whereas peripheral and feeder connections did not differ. Adjusted for the total connectivity of individual brains, we observed an altered distribution of connections between the rich club and periphery. Specifically, in patients with PPMS, we observed a lower density of rich-club connections compared with controls, whereas peripheral connectivity was relatively increased, which might be due to a lower extent of connectivity loss in the periphery compared with the rich-club or might result from compensatory peripheral rewiring. Our adjustment strategy demonstrates that the observed loss of rich-club connections cannot be explained solely by the global loss of connectivity but indicates a disease-specific pattern. Here, reduced rich-club connectivity was associated with T2 lesion load and gray matter volume, connecting our findings to previous observations.[15] Moreover, we observed a correlation of the change in

rich-club connectivity with clinical measures of mobility, hand function, and cognition in our patients.

Alterations to the distribution of connections between rich-club and peripheral nodes have also been observed in other neuropsychiatric diseases and support a disease specificity of distinctive patterns. In migraine patients, an increased number of feeder connections is associated with a higher network efficiency and suspected to cause a higher integration of subnetworks involved in pain processing.[10] However, patients with schizophrenia show reduced rich-club connectivity,[25] and cognitive decline and reduced general function are associated with a pronounced loss of rich-club connections over 3 years.[9] Predominantly neurodegenerative diseases such as Parkinson disease seem to be associated with a pronounced loss of peripheral and feeder connections.[11,26] Within this context, our findings indicate that diffuse perturbations of brain connectivity in PPMS result in a pronounced loss of connectivity within the rich club, and that the overall pattern of connectivity loss differs from primarily neurodegenerative diseases. However, this cross-sectional study does not allow to distinguish between the impact of inflammatory and neurodegenerative mechanisms on the assessed connectivity loss.

This interpretation is supported by data indicating that atrophy appears to follow nonrandom patterns in MS correlated with cognitive impairment and disability.[12] Most of the patterns include the insula, which belongs to the rich-club regions. Moreover, a close correlation between T2 lesions and reduced local efficiency of the insula has been described before,[15] and the affection of hub regions in early RRMS has recently been confirmed in structural and functional connectomes.[27] These findings support our observation that PPMS affects particularly the regions of the brain with a prominent and integrative role in the structural connectome, whereas peripheral connections are less compromised, preserved, or even rewired due to neurorepair. A longitudinal study of fMRI connectivity found a compensatory upregulation in early disease stages without relevant disability.[28] A global loss of connectivity was observed in more disabled patients and correlated with accumulation of disability. Cross-sectional studies support the observation that functional reorganization in MS is complex and leads to different patterns of activation and deactivation related to disability.[29] However, the benefit of this reorganization is questionable.[30] Recruitment of additional neural resource might be inefficient and rather maladaptive than adaptive.[30]

The topology of network reorganization can as well be deduced by contrasting alterations in the large-scale functional networks.[31] The default mode network is considered to represent a backbone of structural-functional organization and shows a heterogeneous pattern of activation and deactivation in MS.[32] Altered default mode connectivity contrasts the connectivity in more peripheral networks, adding further evidence for inverse effects in hubs and the periphery.[31] However, it remains an unresolved issue how reorganization of functional connectivity needs to be interpreted and what the underlying pathologic or repair mechanisms are. Moreover, it is unknown how these functional changes translate into altered structural connectivity. The cross-sectional nature of our study does not allow determining when the shift from rich-club to peripheral connectivity occurs. However, preliminary data in RRMS indicate that the shift toward more peripheral connectivity is detectable within a time frame of 6 months and might be reduced by an exercise intervention.[33] A cross-sectional study in RRMS found also an increased structural connectivity on a local level.[34] Taking the functional data into account, one might hypothesize that a continuous loss of rich-club connectivity can only be compensated by peripheral connections in the early phase.

In contrast to our rich-club analyses, conventional global graph metrics did not differ between patients and controls. The insensitivity of global graph metrics has been described before. For example, they were not able to separate comatose patients from HCs in an fMRI study, while hub regions showed a clear loss in connectivity.[35] These findings support our interpretation that PPMS does not lead to major topological changes but rather to subtle alterations of the brain network.

Our findings are of explorative nature and need further validation. The sample size is relatively small, but in line with similar studies investigating rich-club connectivity.[10,11,26] The study was sufficiently powered to detect alterations in the rich-club connectivity, but was too small to investigate the association with other MRI metrics in depth. For example, we did not detect a difference in white matter volume between patients and controls. Moreover, we could not apply model selection in multivariate statistics to determine the specificity of rich-club alterations for disability in comparison with other MRI measurements. Concerning the mechanisms behind our observations, our interpretations remain hypothetical, as we did not investigate longitudinal changes. Not including relapsing-remitting patients limits the generalization of our findings, but we were primarily interested in neurodegenerative aspects of MS and thus aimed to restrict the influence of acute inflammatory disease activity as much as possible by studying a PPMS cohort. However, especially spinal cord

pathology in this patient group might influence disability by means of the EDSS and mobility assessment and make the interpretation of our association results more difficult. Furthermore, the applied method to reconstruct connectomes shares some inherent limitations. Although the method is well accepted, it may be affected by methodological and disease-specific aspects, such as the undistinguishable, but heterogenic histopathology of MS lesions.[36,37] MS lesions affect the tractography results such as they may underestimate true structural connectivity.[38] However, false-negative connections are known to have a lower impact on the network topology than false-positive connections,[36] and in our data set, the global connectivity did not differ between patients and controls. Our analysis followed the original analysis of the rich club that restricted the topological analyses to cortical regions.[6,25] Thus, we cannot conclude about the role of subcortical gray matter or the cerebellum in the rich-club topology.

In conclusion, PPMS seems to induce a loss of structural connections between important brain regions. Our findings emphasize to interpret the impairment of rich-club connections as disease specific and disability related. Thus, rich-club connectivity is a promising indicator for understanding and monitoring the patterns and mechanisms of neurodegeneration in PPMS.

## AUTHOR CONTRIBUTIONS

Study concept and design: J.-P.S., S.H., B.C., C. Heesen, G.T., and S.S. Acquisition, analysis, or interpretation of data: J.-P.S., S.H., B.C., N.W., K.L.Y., C. Hilgetag, C.G., C. Heesen, G.T., and S.S. Drafting of the manuscript: J.-P.S. and S.H. Critical revision of the manuscript for important intellectual content: J.-P.S., S.H., B.C., N.W., K.L.Y., C. Hilgetag, C.G., C. Heesen, G.T., and S.S. Statistical analysis: J.-P.S., S.H., B.H., G.T., and S.S. Study supervision: J.-P.S., K.L.Y., S.H., and C. Heesen.


## STUDY FUNDING

Data collection was partially supported by grants from Merck Serono and Novartis. The German Ministry for Education and Research supported the work (BMBF, SFB 936/A1, C1, C2, Z3, and TRR 169/A2).


## DISCLOSURE

J.-P. Stellmann served on the scientific advisory board for Genzyme; received travel funding and/or speaker honoraria from Genzyme, Biogen, and Novartis; and received research support from Merck Serono and Biogen. S. Hodecker received travel funding from Genzyme and Roche. B. Cheng, N. Wanke, K.L. Young, and C. Hilgetag report no disclosures and received research support from DFG SFB and DFG TRR. C. Gerloff served on the scientific advisory board for Bayer Vita, Boehringer Ingelheim, EBS Technologies, Silk Road Medical, Acticor Biotech, Amgen, and Prediction Bioscience; received travel funding and/or speaker honoraria from Bayer Vital, Boehringer Ingelheim, Biogen, ev3/Covidien, GlaxoSmithKline, Grifols, Inomed, Lundbeck, Nexstim, Pfizer, Sanofi Aventis, UCB, and Merck Serono; served on the editorial board for INFO Neurologie Psychiatrie and Aktuelle Neurologie; was editor of the textbook "Therapie und Verlauf Neurologischer Erkrankungen"; consulted for EBS Technologies; and received research support from Merz, Novartis, NeuroConn, DFG, BMBF/DFG, EU, DFG: TRR, Wegener Foundation, Movement Disorders Science, Schilling Foundation, and Werner-Otto-Foundation. C. Heesen received speaker honoraria from Biogen, Merck, Genzyme, and Novartis; is on the editorial board for International Journal of MS Care; and received research support from Genzyme, Sanofi Aventis, Biogen, Novartis, Roche, Merck, and German Ministry of Research. G. Thomalla served on the scientific advisory board for TEA Stroke Trial; received travel funding and/or speaker honoraria from Bayer, Boehringer Ingelheim, Daiichi Sankyo, and Bristol-Myers Squibb/Pfizer; consulted for Acandis and GlaxoSmithKline; and received research support from the European Union, Deutsche Forschungsgesellschaft, and Corona Foundation. S. Siemonsen reports no disclosures. Go to Neurology.org/nn for full disclosure forms.


*Received December 12, 2016. Accepted in final form May 17, 2017.*


## REFERENCES


1. Dendrou CA, Fugger L, Friese MA. Immunopathology of multiple sclerosis. Nat Rev Immunol 2015;15:545–558.
2. Hauser SL, Chan JR, Oksenberg JR. Multiple sclerosis: prospects and promise. Ann Neurol 2013;74:317–327.
3. Rovira À, Wattjes MP, Tintoré M, et al. Evidence-based guidelines: MAGNIMS consensus guidelines on the use of MRI in multiple sclerosis—clinical implementation in the diagnostic process. Nat Rev Neurol 2015;11:471–482.
4. Kaiser M. The potential of the human connectome as a biomarker of brain disease. Front Hum Neurosci 2013;7:484.
5. Griffa A, Baumann PS, Thiran JP, Hagmann P. Structural connectomics in brain diseases. Neuroimage 2013;80:515–526.
6. van den Heuvel MP, Sporns O. Rich-club organization of the human connectome. J Neurosci 2011;31:15775–15786.
7. Cao M, He Y, Dai Z, et al. Early development of functional network segregation revealed by connectomic analysis of the preterm human brain. Cereb Cortex 2016;27:1949–1963.
8. de Reus MA, van den Heuvel MP. The parcellation-based connectome: limitations and extensions. Neuroimage 2013;80:397–404.
9. Collin G, de Nijs J, Hulshoff Pol HE, Cahn W, van den Heuvel MP. Connectome organization is related to longitudinal changes in general functioning, symptoms and IQ in chronic schizophrenia. Schizophr Res 2016;173:166–173.
10. Li K, Liu L, Yin Q, et al. Abnormal rich club organization and impaired correlation between structural and functional connectivity in migraine sufferers. Brain Imaging Behav 2017;11:526–540.
11. Daianu M, Mezher A, Mendez MF, Jahanshad N, Jimenez EE, Thompson PM. Disrupted rich club network in behavioral variant frontotemporal dementia and early-onset Alzheimer's disease. Hum Brain Mapp 2016;37:868–883.
12. Steenwijk MD, Geurts JJG, Daams M, et al. Cortical atrophy patterns in multiple sclerosis are non-random and clinically relevant. Brain 2016;139:115–126.
13. Tewarie P, Schoonheim MM, Schouten DI, et al. Functional brain networks: linking thalamic atrophy to clinical disability in multiple sclerosis, a multimodal fMRI and MEG Study. Hum Brain Mapp 2015;36:603–618.
14. Li Y, Jewells V, Kim M, et al. Diffusion tensor imaging based network analysis detects alterations of neuroconnectivity in patients with clinically early relapsing-remitting multiple sclerosis. Hum Brain Mapp 2013;34:3376–3391.
15. He Y, Dagher A, Chen Z, et al. Impaired small-world efficiency in structural cortical networks in multiple sclerosis associated with white matter lesion load. Brain 2009;132:3366–3379.

16. Shu N, Liu Y, Li K, et al. Diffusion tensor tractography reveals disrupted topological efficiency in white matter structural networks in multiple sclerosis. Cereb Cortex 2011;21:2565–2577.
17. Polman CH, Reingold SC, Banwell B, et al. Diagnostic criteria for multiple sclerosis: 2010 revisions to the "McDonald criteria." Ann Neurol 2011;69:292–302.
18. Fischer JS, Rudick RA, Cutter GR, Reingold SC. The multiple sclerosis functional composite measure (MSFC): an integrated approach to MS clinical outcome assessment. Mult Scler 1999;5:244–250.
19. Drake A, Weinstock-Guttman B, Morrow S, Hojnacki D, Munschauer F, Benedict R. Psychometrics and normative data for the multiple sclerosis functional composite: replacing the PASAT with the symbol digit modalities test. Mult Scler 2010;16:228–237.
20. Fischl B. FreeSurfer. Neuroimage 2012;62:774–781.
21. Welton T, Kent DA, Auer DP, Dineen RA. Reproducibility of graph-theoretic brain network metrics: a systematic review. Brain Connect 2015;5:193–202.
22. Opsahl T, Colizza V, Panzarasa P, Ramasco JJ. Prominence and control: the weighted rich-club effect. Phys Rev Lett 2008;101:1–4.
23. Opsahl T. Structure and Evolution of Weighted Networks. London: University of London (Queen Mary College), London, UK; 2009.
24. Csardi G, Nepusz T. The igraph software package for complex network research. Inter J Complex Syst 2006; 1695:1695.
25. Collin G, Kahn RS, De Reus MA, Cahn W, Van Den Heuvel MP. Impaired rich club connectivity in unaffected siblings of schizophrenia patients. Schizophr Bull 2014;40: 438–448.
26. Li C, Huang B, Zhang R, et al. Impaired topological architecture of brain structural networks in idiopathic Parkinson's disease: a DTI study. Brain Imaging Behav 2016; 22:1–16.
27. Shu N, Duan Y, Xia M, et al. Disrupted topological organization of structural and functional brain connectomes in clinically isolated syndrome and multiple sclerosis. Sci Rep 2016;6:29383.
28. Faivre A, Robinet E, Guye M, et al. Depletion of brain functional connectivity enhancement leads to disability progression in multiple sclerosis: a longitudinal resting-state fMRI study. Mult Scler J 2016;22:1695–1708.
29. Rocca MA, Valsasina P, Meani A, Falini A, Comi G, Filippi M. Impaired functional integration in multiple sclerosis: a graph theory study. Brain Struct Funct 2016; 221:115–131.
30. Enzinger C, Pinter D, Rocca MA, et al. Longitudinal fMRI studies: exploring brain plasticity and repair in MS. Mult Scler J 2016;22:269–278.
31. Rocca MA, Valsasina P, Martinelli V, et al. Large-scale neuronal network dysfunction in relapsing-remitting multiple sclerosis. Neurology 2012;79:1449–1458.
32. Zhou F, Zhuang Y, Gong H, et al. Altered inter-subregion connectivity of the default mode network in relapsing remitting multiple sclerosis: a functional and structural connectivity study. PLoS One 2014;9:e101198.
33. Hodecker SC, Siemonsen S, Kjølhede T, et al. Physical exercise-related changes in structural connectome architecture in patients with relapsing-remitting multiple sclerosis. Mult Scler J 2016;22:35.
34. Fleischer V, Gröger A, Koirala N, et al. Increased structural white and grey matter network connectivity compensates for functional decline in early multiple sclerosis. Mult Scler 2017;23:432–441.
35. Achard S, Delon-Martin C, Vértes PE, et al. Hubs of brain functional networks are radically reorganized in comatose patients. Proc Natl Acad Sci USA 2012;109: 20608–20613.
36. Zalesky A, Fornito A, Cocchi L, Gollo LL, van den Heuvel MP, Breakspear M. Connectome sensitivity or specificity: which is more important? Neuroimage 2016;142:407–420.
37. Bastiani M, Shah NJ, Goebel R, Roebroeck A. Human cortical connectome reconstruction from diffusion weighted MRI: the effect of tractography algorithm. Neuroimage 2012;62:1732–1749.
38. Droby A, Fleischer V, Carnini M, et al. The impact of isolated lesions on white-matter fiber tracts in multiple sclerosis patients. Neuroimage Clin 2015;8:110–116.

**Reduced rich-club connectivity is related to disability in primary progressive MS**

Jan-Patrick Stellmann, Sibylle Hodecker, Bastian Cheng, et al.

*Neurol Neuroimmunol Neuroinflamm* 2017;4;
DOI 10.1212/NXI.0000000000000375